Glyoxylate detoxification is an essential function of malate synthase required for carbon assimilation in *Mycobacterium tuberculosis*

Susan Puckett[a], Carolina Trujillo[a], Zhe Wang[b], Hyungjin Eoh[b,1], Thomas R. Ioerger[c], Inna Krieger[c], James Sacchettini[c], Dirk Schnappinger[a], Kyu Y. Rhee[b,2], and Sabine Ehrt[a,2]

[a]Department of Microbiology and Immunology, Weill Cornell Medical College, New York, NY 10021; [b]Department of Medicine, Weill Cornell Medical College, New York, NY 10021; and [c]Department of Biochemistry and Biophysics, Texas A&M University, College Station, TX 77843

Edited by William R. Jacobs Jr., Albert Einstein College of Medicine, Howard Hughes Medical Institute, Bronx, NY, and approved February 3, 2017 (received for review October 26, 2016)

The glyoxylate shunt is a metabolic pathway of bacteria, fungi, and plants used to assimilate even-chain fatty acids (FAs) and has been implicated in persistence of *Mycobacterium tuberculosis* (*Mtb*). Recent work, however, showed that the first enzyme of the glyoxylate shunt, isocitrate lyase (ICL), may mediate survival of *Mtb* during the acute and chronic phases of infection in mice through physiologic functions apart from fatty acid metabolism. Here, we report that malate synthase (MS), the second enzyme of the glyoxylate shunt, is essential for in vitro growth and survival of *Mtb* on even-chain fatty acids, in part, for a previously unrecognized activity: mitigating the toxicity of glyoxylate excess arising from metabolism of even-chain fatty acids. Metabolomic profiling revealed that MS-deficient *Mtb* cultured on fatty acids accumulated high levels of the ICL aldehyde endproduct, glyoxylate, and increased levels of acetyl phosphate, acetoacetyl coenzyme A (acetoacetyl-CoA), butyryl CoA, acetoacetate, and β-hydroxybutyrate. These changes were indicative of a glyoxylate-induced state of oxaloacetate deficiency, acetate overload, and ketoacidosis. Reduction of intrabacterial glyoxylate levels using a chemical inhibitor of ICL restored growth of MS-deficient *Mtb*, despite inhibiting entry of carbon into the glyoxylate shunt. In vivo depletion of MS resulted in sterilization of *Mtb* in both the acute and chronic phases of mouse infection. This work thus identifies glyoxylate detoxification as an essential physiologic function of *Mtb* malate synthase and advances its validation as a target for drug development.

tuberculosis | metabolism | malate synthase | glyoxylate detoxification

The unusual evolution of *Mycobacterium tuberculosis* (*Mtb*) within humans as both host and reservoir has shaped its pathogenicity around adaptation of its carbon and energy metabolism to the diverse yet specific array of microenvironments encountered within human hosts (1). Current evidence indicates that *Mtb* can be found inside lipid-rich macrophages and in cavities, suggesting that these environments provide the pathogen with nutrients that facilitate persistence (2, 3). Consistent with this evidence, multiple *Mtb* genes involved in fatty acid (FA) and lipid uptake and catabolism have been shown to be essential to establish and maintain chronic infections in mice (4–8). Together, such studies have directed considerable attention to pathways of lipid catabolism as a key determinants of *Mtb*'s pathogenicity and sources of potential drug targets (9).

Our understanding of *Mtb*'s metabolic pathways however remains rudimentary. This knowledge derives in large part from the functions of orthologous genes conserved in other organisms. Though powerful for its assignment of biochemical functions, comparative genomic approaches neglect potentially important differences in the ecologic niches and selective pressures that genes have evolved to serve. One emerging and prominent example of such dissociation is exemplified by our understanding of the function of *Mtb*'s glyoxylate shunt. The glyoxylate shunt consists of two enzymatic reactions catalyzed by isocitrate lyase (ICL) and malate synthase (MS) (Fig. S1). The first enzyme in the pathway, ICL, cleaves isocitrate into glyoxylate and succinate. The second enzyme, MS, catalyzes the conversion of glyoxylate and acetyl coenzyme A (acetyl-CoA) into malate and CoA (Fig. S1). Together, these enzymes enable bacteria, plants, and fungi to assimilate biomass when cultured on even-chain fatty acids by bypassing the oxidative decarboxylation of two carbon units associated with the TCA cycle. Early work showed that ICL is critical for *Mtb*'s ability to replicate and persist in mice (4, 7), whereas genome-wide transposon mutagenesis studies and the failure to generate a MS mutant suggested MS to be essential for growth in vitro (10, 11). Based on these data, the essentiality of these enzymes was largely ascribed to their canonical role in carbon assimilation and anaplerosis.

Recent work, however, showed that *Mtb* requires ICL for functions apart from carbon assimilation. These include resistance to a variety of stresses relevant to infection, such as hypoxia, starvation, and a broad spectrum of antibiotics (12–15). ICL also functions as a methylisocitrate lyase in the methylcitrate cycle, which is critical for metabolism and detoxification of odd-chain fatty acids (16, 17). Moreover, loss of methylisocitrate lyase activity in ICL-deficient *Mtb* was specifically shown to mediate the bactericidal essentiality of ICL due to previously unrecognized roles of the methylcitrate cycle in homeostasis of *Mtb*'s intrabacterial pH and membrane potential (13). Based on these findings, we sought to investigate the essentiality and role of MS in the virulence of *Mtb*.

Significance

A better understanding of essential processes in *Mycobacterium tuberculosis* (*Mtb*) is required for the development of new chemotherapeutics. Isocitrate lyase (ICL) and malate synthase (MS) function in the glyoxylate shunt, a pathway required by *Mtb* to metabolize fatty acids (FAs). Here, we demonstrate that *Mtb* MS enables growth and survival on fatty acids through its ability to simultaneously detoxify a metabolic byproduct arising from the initial assimilation of acetyl coenzyme A (acetyl-CoA), glyoxylate, while assimilating a second molecule of acetyl-CoA. We further show that MS depletion during acute and chronic mouse infections kills *Mtb*. These studies expand our fundamental understanding of the glyoxylate shunt and biologically validate MS as an attractive drug target in *Mtb*.

Author contributions: S.P., C.T., Z.W., H.E., T.R.I., D.S., K.Y.R., and S.E. designed research; S.P., C.T., Z.W., H.E., and T.R.I. performed research; I.K. and J.S. contributed new reagents/analytic tools; S.P., C.T., Z.W., H.E., T.R.I., D.S., K.Y.R., and S.E. analyzed data; and S.P., K.Y.R., and S.E. wrote the paper.

The authors declare no conflict of interest.

This article is a PNAS Direct Submission.

[1]Present address: Department of Molecular Microbiology and Immunology, Keck School of Medicine, University of Southern California, Los Angeles, CA 90033.

[2]To whom correspondence may be addressed. Email: sae2004@med.cornell.edu or kyr9001@med.cornell.edu.

This article contains supporting information online at www.pnas.org/lookup/suppl/doi:10.1073/pnas.1617655114/-/DCSupplemental.

MS catalyzes the conversion of glyoxylate and acetyl-CoA into malate and CoA (Fig. S1) and is not known to have secondary metabolic functions. The crystal structure and catalytic mechanism of MS have been extensively studied (18, 19) and potent inhibitors of the enzyme have been developed (20). MS inhibitors killed *Mtb* in culture and reduced the bacterial load in a mouse model of acute infection (20). Unexpectedly, the bactericidal activity was not restricted to bacteria metabolizing acetate but also glucose, suggesting that MS might be required for survival of *Mtb* independently of the carbon source, or that these inhibitors target additional enzymes. In this work, we identified conditions that rendered MS dispensable for growth of *Mtb*, and allowed us to generate a MS-deficient strain. This deletion mutant and a conditional knockdown strain helped define the specific metabolic consequences associated with loss of MS activity, the essentiality of MS during acute and chronic mouse infections, and a unique physiologic role of MS unrelated to carbon assimilation, not shared by ICL-deficient *Mtb*.

Results

MS Is Required for *Mtb* Virulence in Mice. We first sought to evaluate whether MS is important for growth and persistence of *Mtb* in vivo. Chemical inhibition of MS impaired the ability of *Mtb* to establish an acute infection in mice (20). However, whether MS is required for persistence during the chronic phase of infection had not been determined. Therefore, we generated a mutant in which MS could be depleted at any time postinfection. In this dual control (DUC) strain, MS is transcriptionally silenced and proteolytically degraded by addition of anhydrotetracycline (atc) or doxycycline (doxy), as previously described (21). To achieve this objective, we generated a strain that contained a second copy of *glcB*, which encodes MS, on a streptomycin resistance-conferring plasmid integrated at the attachment site of the mycobacteriophage L5 (*attL5*) in the chromosome of wild-type (WT) *Mtb* Erdman. Next, we replaced the native *glcB* gene with a hygromycin resistance cassette and confirmed deletion of *glcB* by Southern blot (Fig. S2 *A* and *B*). Plasmids in the *attL5* site can be efficiently replaced by another plasmid that also integrates into *attL5* and can be selected for with a different antibiotic (22). We transformed the mutant with a plasmid that conferred zeocin resistance and contained DAS (aspartate-alanine-serine)-tagged *glcB* expressed from the tetracycline (tet)-operator containing promoter P750, and reverse tet repressor driven by a constitutive promoter. In addition, the mutant was transformed with a plasmid that integrates in the tweety phage attachment site and expresses the SspB adapter protein—responsible for targeting MS-DAS to the ClpP protease—under control of the wild-type tet repressor. Treatment of *Mtb glcB*-DUC with atc reduced abundance of MS to undetectable levels (Fig. S2*C*) and inhibited growth in carbon-defined media with acetate as carbon source (Fig. S3). This experiment established that *glcB* expression was regulated in an atc-dependent manner. We infected mice with *glcB*-DUC and fed them doxy to inactivate MS at different time points during and after establishment of infection (Fig. 1 *A* and *B*). In response to doxy treatment, titers of *glcB*-DUC declined in lungs and spleens at all time points tested. This decline was accompanied by a significant reduction in lung pathology. In mice treated with doxy on day 35, when the lungs contained numerous lesions, hardly any lesions were detectable anymore by day 113 (Fig. 1*B*). This experiment confirmed that MS is required for growth of *Mtb* in vivo and demonstrated that MS is also essential for persistence during the chronic phase of mouse infection.

MS Essentiality Depends on the Carbon Source. The essentiality of *Mtb* genes encoding enzymes of central carbon metabolism can be carbon source dependent (6, 8, 23, 24). Such dependence may help explain apparent discrepancies in transposon mutagenesis-based studies of gene essentiality, including for *glcB* (10, 25).

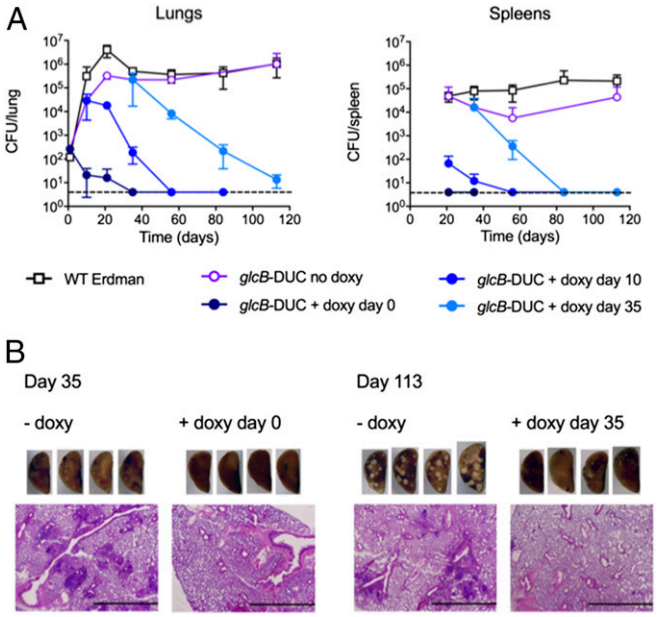

Fig. 1. *Mtb* requires MS for growth and persistence in mice. (*A*) Bacterial burden in lungs and spleens of mice infected with WT *M. tuberculosis* Erdman and the *glcB*-DUC strain. Mice infected with *glcB*-DUC received doxy-containing food from the day of infection (day 0), day 10, day 35, or not at all as indicated. Lung and spleen homogenates were cultured to determine bacterial burden at the indicated time points postinfection. Data are means ± SD of four mice per time point (except for *glcB*-DUC isolated from spleens of untreated mice on day 56, three mice). Data are representative of two independent experiments. (*B*) Gross lung pathology and hematoxylin and eosin stained lung sections isolated at day 35 and day 113 from mice infected with *glcB*-DUC and given doxy to deplete MS at the indicated times. (Scale bar, 2 mm.)

Accordingly, we observed that MS-depleted *glcB*-DUC was able to grow in media with glucose as a sole carbon source (Fig. S3). Because previous attempts to generate a *glcB* knockout on standard media had failed, we investigated whether changing the media composition would permit genetic deletion of *Mtb glcB*. Using the mutant that contained a single copy of *glcB* in the *attL5* site, we attempted to remove *glcB* by transforming it with a plasmid lacking *glcB* and conferring kanamycin resistance. Transformants were cultured on standard *Mtb* agar plates containing kanamycin for selection and glucose, glycerol and oleic acid as carbon sources, or glucose and glycerol but no oleic acid. Kanamycin-resistant colonies appeared only on media lacking oleic acid. This *glcB* knockout (Δ*glcB*) did not express MS (Fig. S2*C*) and it recapitulated the sensitivity toward oleic acid when recultured on agar plates (Fig. 2*A*). In liquid media, Δ*glcB* also had a significant growth defect when oleic acid was present, but grew like WT *Mtb* when cultured only with glucose and glycerol (Fig. 2*A*). In contrast, growth of ICL-deficient *Mtb* (Δ*icl1/2*) was less impaired than Δ*glcB Mtb* in oleic-acid–containing medium, and not improved by omission of oleic acid. This sensitivity was not unique to oleic acid, because growth of Δ*glcB* was also inhibited by cholesterol, a physiologically relevant carbon source that is catabolized into acetyl-CoA, propionyl-CoA, and pyruvate (26) (Fig. 2*B*). Although cholesterol supported growth of WT and enhanced its growth with glucose, it was toxic to Δ*glcB*, suppressing its growth even in the presence of glucose. This finding demonstrated that, although MS is not essential for growth in all conditions, it is required to resist fatty-acid–associated toxicity.

To further assess the phenotype of Δ*glcB* in host-relevant conditions, we quantified bacterial burden over time in bone-marrow–derived macrophages (BMDMs) and in the mouse model. We found that Δ*glcB* failed to replicate and survive in

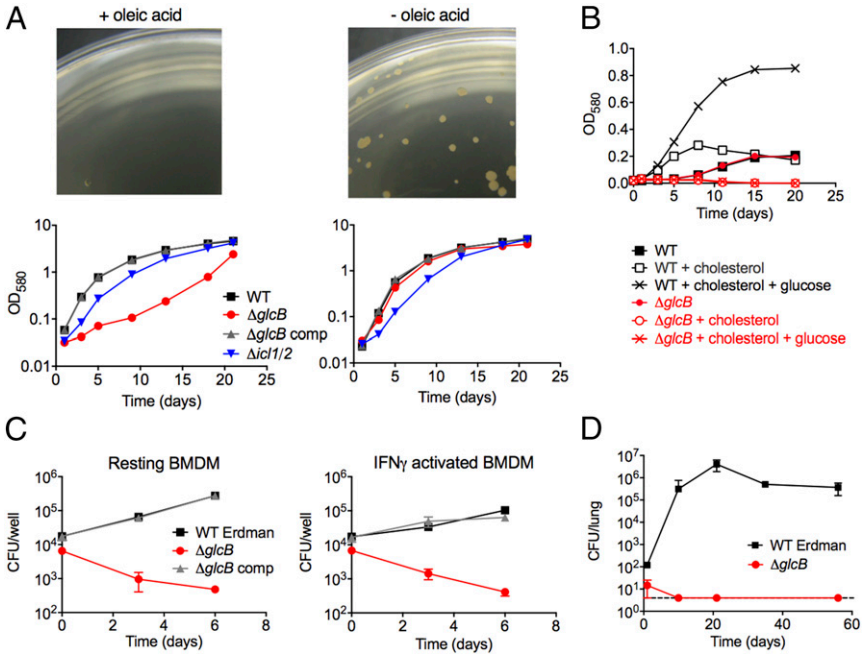

Fig. 2. Impact of MS deficiency on growth in vitro, in macrophages and in mice. (*A*, *Top*) Images depict growth of Δ*glcB* on agar plates containing 0.2% glucose and 0.5% glycerol, with or without 0.006% oleic acid (as indicated). Graphs below show growth of WT Erdman (WT), Δ*glcB*, the Δ*glcB* complemented strain, and Δ*icl1*Δ*icl2* in 7H9 base media containing 0.2% glucose and 0.5% glycerol with or without 0.006% oleic acid. (*B*) Growth of WT and Δ*glcB* in cholesterol base media without added carbon or with 0.01% cholesterol or with 0.01% cholesterol and 0.2% glucose. Data are representative of two independent experiments. (*C*) Growth and survival of WT, Δ*glcB*, and the Δ*glcB* complemented *Mtb* strains in resting and IFN-γ activated mouse bone-marrow–derived macrophages (BMDMs). Activated macrophages were treated with 30 ng/mL IFN-γ 1 d before infection. Data are representative of two independent experiments. (*D*) Bacterial burden in lungs of mice infected with WT and Δ*glcB*. Lung homogenates were cultured on Δ*glcB* growth-permissive media to determine bacterial burden at the indicated time points postinfection. No cfus were detected in spleens of Δ*glcB*-infected mice at any of the time points tested. Data are means ± SD of four mice per time point. Data are representative of two independent experiments.

resting and in IFN-γ–activated macrophages, a cell type critical for *Mtb*'s intracellular lifestyle within the host (Fig. 2*C*). Also, mice infected with Δ*glcB* quickly cleared the infection (Fig. 2*D*). At 10 d after infection no bacteria were detectable in lungs, whereas WT Erdman had expanded by over four orders of magnitude. Thus, infection with Δ*glcB* confirmed the essentiality of MS for growth and survival in macrophages and in the acute phase of mouse infection.

MS Is Required to Resist Both Even- and Odd-Chain Fatty-Acid–Associated Toxicity. To investigate the fatty acid sensitivity of Δ*glcB*, we assessed growth in carbon-defined minimal media. Although even-chain fatty acids are broken down into acetyl-CoA by β-oxidation, metabolism of long, odd-chain fatty acids (and cholesterol) gives rise to both acetyl- and propionyl-CoA. We therefore tested the impact of both even- and odd-chain fatty acid carbon sources on growth. Δ*glcB* grew indistinguishably from WT with glucose or glycerol as a sole carbon source, but failed to grow with acetate or butyrate (Fig. 3*A* and Fig. S4*A*). Δ*glcB* also failed to grow in media with propionate. Moreover, the addition of glucose failed to rescue growth of Δ*glcB* in media containing acetate, propionate, or valerate (Fig. 3*B*).

Previous work showed that *Mtb* can metabolize propionate through both TCA-cycle–dependent and –independent pathways. The former, TCA-cycle–dependent pathway, known as the methylcitrate cycle, converts propionyl-CoA into pyruvate and succinate via condensation with oxaloacetate, followed by a dehydration/isomerization and cleavage reaction, whereas the latter, TCA-cycle–independent methylmalonyl-CoA pathway, converts propionyl-CoA into succinyl-CoA via a carboxylation reaction followed by a vitamin B_{12}-dependent isomerization reaction (27) (Fig. S1). We found that addition of 10 μg/mL vitamin B_{12} restored wild-type levels of growth to Δ*glcB Mtb* in the presence of odd-, but not even-chain fatty acids, suggesting that lack of MS impairs metabolism of propionyl CoA via effects on the TCA cycle. Consistent with this view, growth with valerate, which gives rise to both acetyl- and propionyl-CoA, was only enhanced but not rescued by vitamin B_{12}. Unexpectedly, vitamin B_{12} suppressed growth of Δ*glcB Mtb* in 0.05% acetate and 0.2% glucose, a phenotype that requires further investigation. Notwithstanding, these results indicated that the fatty-acid–specific growth defects of Δ*glcB Mtb* are mediated by effects on levels of TCA cycle intermediates.

Focusing on the role of *Mtb* MS in acetate metabolism, we noted that, although high concentrations of acetate inhibited growth of both WT and Δ*glcB Mtb*, Δ*glcB* was consistently more vulnerable to acetate than WT (Fig. 3*C* and Fig. S4*B*). In contrast, low concentrations of acetate surprisingly appeared to enhance growth of Δ*glcB* over that on glucose alone. Indeed, although 0.2% acetate completely suppressed growth of Δ*glcB* in the presence of 0.2% glucose, 0.025% acetate enhanced growth (Fig. 3*C*). These results suggested that Δ*glcB* is able to cocatabolize glucose and acetate at low acetate concentrations but becomes vulnerable to a dominant negative toxicity at higher concentrations of acetate (Fig. 3*D* and Fig. S4*B*). Indeed, the kinetics of Δ*glcB* death were dependent on the acetate concentration and, unexpectedly, exacerbated by glucose at acetate concentrations of 0.2%, resulting in a 4 $\log_{10}$ reduction in viability during 30 d of incubation (Fig. 3*D*). As expected, vitamin B_{12} could not rescue growth of Δ*glcB* with 0.05% acetate and 0.2% glucose (Fig. 3*B*). Taken together, these results indicate that MS deficiency renders *Mtb* vulnerable to fatty acids via a dominant negative effect on TCA cycle intermediates.

Glyoxylate Toxicity in MS-Deficient *Mtb*. Although both ICL and MS participate in the same pathway, MS-deficient *Mtb* displayed an increased susceptibility to oleic acid that could not be rescued by

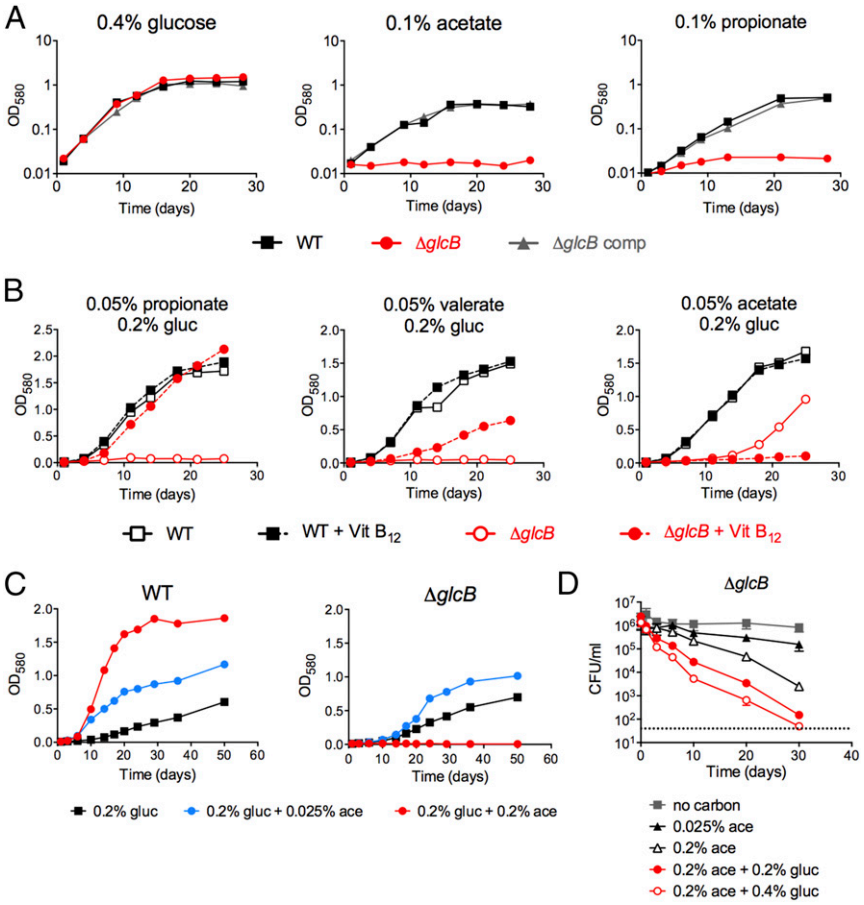

Fig. 3. Fatty acid toxicity in Δ*glcB*. (*A*) Growth of WT, Δ*glcB*, and the Δ*glcB* complemented strains in carbon-defined minimal media with 0.4% glucose, 0.1% acetate, or 0.1% propionate as single carbon sources. (*B*) Growth of WT and Δ*glcB Mtb* strains in the presence or absence of 10 μg/mL vitamin B_{12} with the indicated carbon sources (gluc, glucose). (*C*) Growth of WT and Δ*glcB* in glucose-containing media supplemented with 0%, 0.025%, or 0.2% acetate. (*D*) Cfu quantification of Δ*glcB* incubated in media containing the indicated combinations of acetate and glucose. Data are means ± SD of triplicate cultures; the stippled line denotes the limit of detection (50 cfu).

glucose and glycerol, which supported partial growth of Δ*icl1/2 Mtb* (Fig. 2*A*). We therefore sought to functionally determine whether the increased vulnerability of Δ*glcB Mtb* was due to accumulation of glyoxylate, the direct substrate of MS (and product of ICL), or depletion of malate, a shared downstream product of both ICL and MS. To do so, we tested the impact of ICL inhibition on growth of Δ*glcB* in fatty acids. As shown in Fig. 4*A*, addition of the ICL inhibitor itaconic acid (13) eliminated the growth lag of Δ*glcB* caused by 0.006% oleic acid or 0.05% acetate. Addition of itaconic acid to plates containing oleic acid similarly enabled growth of Δ*glcB* in a dose-dependent manner (Fig. 4*B*). Glyoxylate also inhibited growth of Δ*glcB* with a lower minimal inhibitory concentration (MIC) than against WT *Mtb* specifically in acetate-containing media (Fig. S5). Together, these results thus indicate that the heightened susceptibility of Δ*glcB Mtb* to oleic acid is functionally linked to accumulation of glyoxylate, rather than depletion of malate.

Metabolic Consequences of Malate Synthase Deletion. To directly investigate the metabolic changes associated with growth-permissive and death-inducing conditions, we analyzed metabolite pool sizes in WT and Δ*glcB Mtb* by liquid chromatography-coupled mass spectrometry (LC-MS) before the onset of any

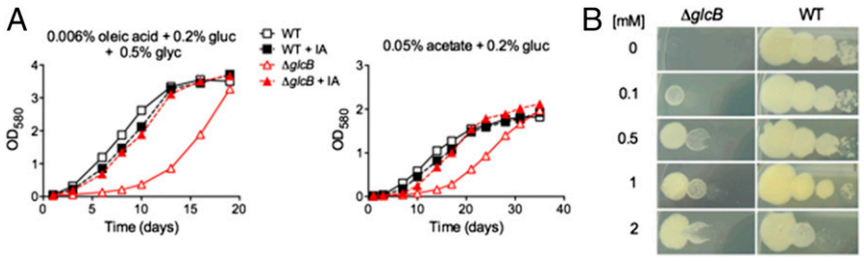

Fig. 4. Glyoxylate toxicity contributes to the fatty acid sensitivity of Δ*glcB*. (*A*) WT and Δ*glcB Mtb* strains were grown with or without 4 mM itaconic acid in 7H9 base media supplemented with 0.006% oleic acid, 0.2% glucose, and 0.5% glycerol or minimal media with 0.05% acetate and 0.2% glucose. (*B*) Serial dilutions of WT and Δ*glcB* cultures were grown on 7H10 agar containing 0.006% oleic acid, 0.2% glucose, and 0.5% glycerol with the indicated concentration of itaconic acid. Data represent two independent experiments.

measurable loss of viability (Fig. 5). Bacteria were grown on filters and exposed to four conditions: (*i*) 0.2% glucose, (*ii*) 0.2% acetate, (*iii*) 0.025% acetate and 0.2% glucose, and (*iv*) 0.2% acetate and 0.2% glucose for 1 d. The most profound difference in metabolite pools size was observed for glyoxylate. In addition, glyoxylate accumulation in death-inducing conditions (0.2% acetate; 0.2% acetate plus 0.2% glucose) was greater than in growth-permissive conditions (0.2% glucose; 0.2% glucose plus 0.025% acetate). Addition of itaconic acid, conversely, reduced the glyoxylate pool size in Δ*glcB* grown on plates containing 0.2% glucose and 0.05% acetate (Fig. S6). However, glyoxylate accumulated in Δ*glcB* in all conditions tested. Indeed, addition of 0.2% acetate to 0.2% glucose significantly enhanced accumulation of glyoxylate, as did addition of 0.025% acetate to 0.2% glucose, which promoted growth of Δ*glcB*. This dissociation suggested that, although perhaps necessary, glyoxylate accumulation alone was not sufficient to mediate growth inhibition or death.

In contrast to the accumulation of metabolites upstream of the MS reaction, levels of downstream metabolites [malate, aspartate (indicative of oxaloacetate)] exhibited reciprocal reductions compared with WT and complemented mutant strains, with magnitudes that correlated with growth inhibition. Levels of succinate, fumarate, and methyl(iso)citrate similarly exhibited deficiencies that were strictly associated with growth inhibition. These results thus corroborate the expected role of *glcB* encoding the only functional MS enzyme in *Mtb* and identify potential downstream mediators and/or reporters of fatty-acid–induced toxicity in Δ*glcB*.

Glyoxylate exists primarily as a gem-diol hydrate in which one carbon is bonded with two hydroxyl groups, but may also exist in an aldehyde form capable of reacting with proteins and DNA within the cell (28, 29). In addition to macromolecular reactivity, glyoxylate can also react with other metabolites such as oxaloacetate and pyruvate, resulting in products that can reduce levels of the corresponding metabolites and/or inhibit enzymes of the TCA cycle (30). Consistent with prior reports of glyoxylate as a competitive inhibitor of pyruvate dehydrogenase (31, 32), we observed increased levels of pyruvate in the MS mutant cultured

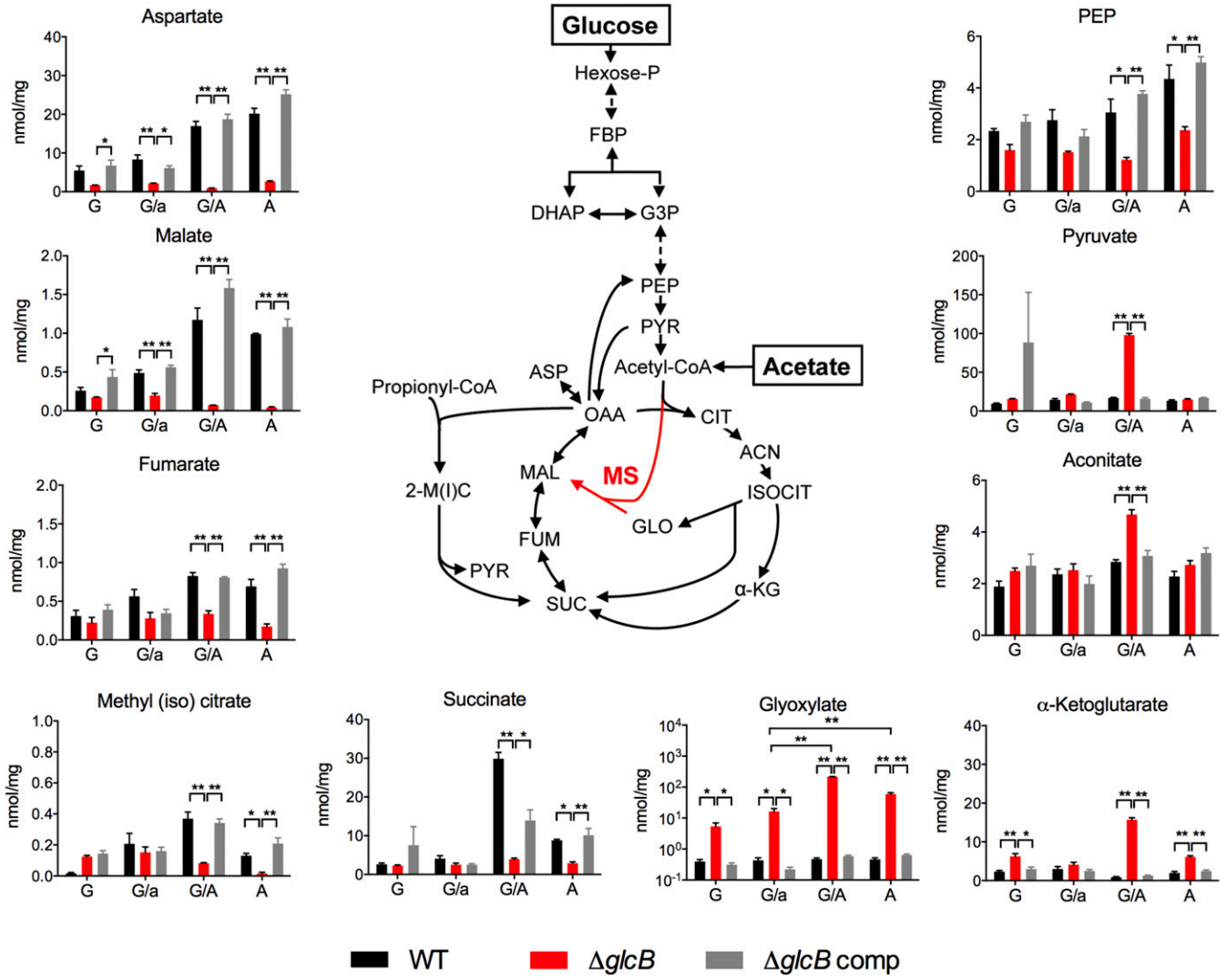

Fig. 5. Metabolic consequences of MS deficiency. Intrabacterial pool sizes of selected metabolites (nmol/mg protein) in the indicated *Mtb* strains after 24-h exposure to Δ*glcB* growth-permissive media containing 0.2% glucose (G) or 0.2% glucose and 0.025% acetate (G/a), or Δ*glcB* bactericidal media containing 0.2% glucose and 0.2% acetate (G/A), or only 0.2% acetate (A). Data are means ± SEM of triplicate samples. Datasets G, G/A, and A are representative of two experiments; G/a was performed once. $*P \leq 0.05$, $**P \leq 0.005$ by one-way ANOVA and Tukey's multiple comparisons test. Abbreviations: 2-M(I)C, 2-methyl(iso)citrate; ACN, *cis*-aconitate; α-KG, alpha-ketoglutarate; ASP, aspartate; CIT, citrate; DHAP, dihydroxyacetone phosphate; FBP, fructose 1,6-bisphosphate; FUM, fumarate; G3P, glyceraldehyde 3-phosphate; GLO, glyoxylate; ISOCIT, isocitrate; MAL, malate; OAA, oxaloacetate; PEP, phosphoenolpyruvate; PYR, pyruvate; and SUC, succinate.

on glucose and acetate (Fig. 5). Owing to their acid lability, we could not directly monitor levels of oxaloacetate or oxalomalate, the condensation product of oxaloacetate and glyoxylate (33, 34). However, using aspartate as a transaminated surrogate, we observed significant deficiencies in Δ*glcB* with magnitudes that correlated with both the presence of a fatty acid and growth inhibition, indicating a relative biochemical deficiency of oxaloacetate in these settings. Moreover, incubation of Δ*glcB* on 0.2% glucose plus 0.2% acetate revealed linked accumulations of glyoxylate and the acetate-derived accumulation products, acetylphosphate, acetoacetyl-CoA, butyryl-CoA, and acetoacetate and β-hydroxybutyrate (neither of which was observed on glucose) supporting a glyoxylate-induced consumption and deficiency of oxaloacetate (Figs. 5 and 6). Consistent with a functional reduction in oxaloacetate levels (13), we also observed that activation of the TCA-cycle–independent (and hence oxaloacetate-sparing) methylmalonyl-CoA pathway enabled growth of Δ*glcB Mtb* on propionate (Fig. 3*B*).

Oxaloacetate serves as both a primary reactant and final product of fatty acid metabolism through the glyoxylate shunt. Lack or deficiency of oxaloacetate results in a reduced capacity to assimilate acetyl CoA, leading to an accumulation of acidic ketone bodies from the condensation of two unassimilated molecules of acetyl-CoA. Consistent with this prediction, we observed matching and specific accumulations of acetoacetyl-CoA, and the corresponding reduced ketone bodies, acetoacetate and β-hydroxybutyrate, as well as accumulations of butyryl-CoA and acetylphosphate, and reciprocal decreases in free CoA pools in MS-deficient *Mtb* cultured in the presence of acetate (Fig. 6). Unfortunately, efforts to rescue MS-deficient *Mtb* from acetate toxicity by functionally replenishing oxaloacetate pools using exogenous oxaloacetate or succinate were unsuccessful, likely due to a combination of inadequate uptake rates and pH-limiting concentrations of metabolites that could be used.

Discussion

This work establishes a critical role for MS in fatty acid resistance and in vivo persistence of *Mtb* and uncovers a physiologic role of MS in *Mtb*. The perceived importance of the glyoxylate shunt for virulence of *Mtb* stems primarily from the essentiality of ICL for in vitro growth on fatty acids and attenuation of ICL-deficient *Mtb* in the acute and chronic phases of a mouse model of pulmonary TB (4, 7). However, the consequences of inactivating ICL are complex as it affects multiple physiologic functions, only some of which are mediated through its canonical role in carbon assimilation. These include two distinct metabolic activities in the glyoxylate shunt and methylcitrate cycle, the latter of which was recently shown to mediate in vitro survival on even- and odd-chain fatty acids, due to critical roles in pH and membrane potential homeostasis (13, 16). Moreover, this work showed that the canonical role of ICL in assimilation of even-chain fatty acids was, in fact, only essential for growth, but not survival, of *Mtb*.

Here, we report that *Mtb*'s MS is essential for survival during the acute and chronic phases of infection in vivo and conditionally essential for survival on fatty acid substrates in vitro. However, this essentiality is mediated by a similarly nonredundant function interlinked with, but distinct from, carbon assimilation—the detoxification of glyoxylate generated by ICL. Strikingly, addition of the ICL inhibitor itaconic acid, which inhibited entry of carbon through the glyoxylate shunt, also alleviated the bactericidal toxicity of fatty acid substrates against Δ*glcB Mtb*, while reducing intrabacterial levels of glyoxylate. It is similarly interesting to note

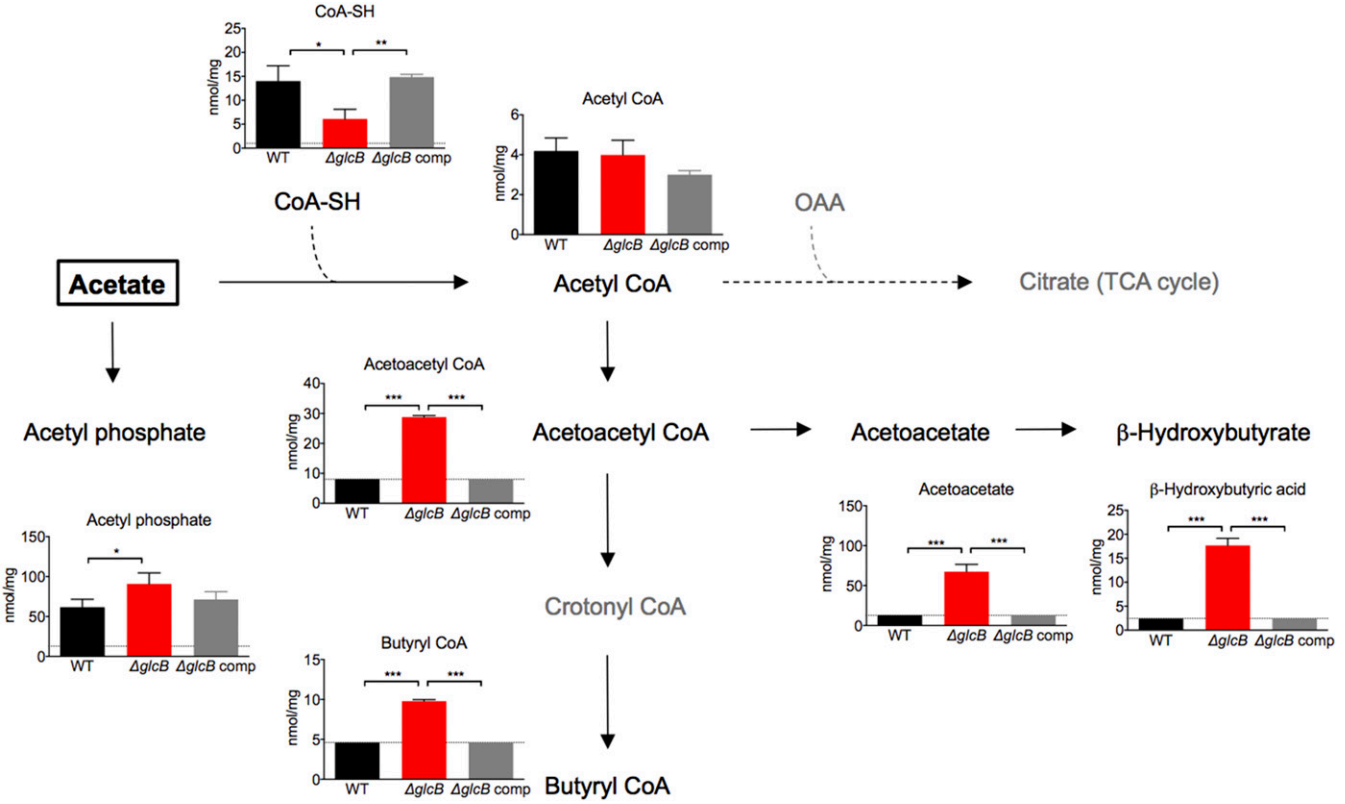

Fig. 6. MS deficiency causes ketoacidosis and CoA deficiency. Intrabacterial pool sizes of acetate-derived metabolites (nmol/mg protein) in the indicated *Mtb* strains after 24-h exposure to 0.2% glucose and 0.2% acetate for 24 h. Data are means ± SD of triplicate samples. Dotted lines indicate the limit of quantification. $*P \leq 0.05$, $**P \leq 0.005$, $***P \leq 0.0005$ by one-way ANOVA and Tukey's multiple comparisons test.

that the specific activity of MS is 6 μmol/min/mg (18), whereas that of ICL is 1.3 μmol/min/mg (35) perhaps pointing to a requirement for increased MS activity.

The specific physiologic mechanism(s) of glyoxylate toxicity remains to be elucidated. However, the discovery of accumulated secondary/alternative products of acetate metabolism, including ketone bodies (a widely recognized biochemical derangement associated with starvation), identify ketoacidosis, and depletion of free CoA as two potential contributory mechanisms. Both acetoacetic acid and β-hydroxybutyric acid are acidic and can promote an intracellular acidosis over time as occurs in humans (36). The specific impact of ketoacidosis in Δ*glcB Mtb* thus awaits further investigation. Recent work by Evans et al. similarly reported the vulnerability of *Mtb* to inhibition of CoA biosynthesis (37).

Glyoxylate toxicity may not be specific to *Mtb*, as a strain of the plant pathogen *Rhodococcus fascians* with a mutation in MS displayed impaired pathogenicity and accumulated glyoxylate (38). In contrast, *Escherichia coli* prevents glyoxylate accumulation via three reactions: (*i*) conversion to malate, (*ii*) reduction to glycolate, or (*iii*) conversion to 3-phosphoglycerate (39, 40). Although the latter two appear to be absent in *Mtb*, *Mtb* is annotated to encode a glycine dehydrogenase capable of catalyzing the unidirectional reductive amination of glyoxylate to glycine (41). Notwithstanding, the data presented here identify a nonredundant role of *Mtb*'s MS in glyoxylate detoxification. Glyoxylate was recently reported to activate isocitrate dehydrogenase in mycobacteria, driving flux through the TCA cycle (42). In agreement, glyoxylate accumulation in the MS mutant was accompanied by a significant increase in pool size of α-ketoglutarate.

It is interesting to note that the impact of acetate on growth of MS-deficient *Mtb* was concentration dependent. Despite inhibiting growth at high concentrations, low concentrations of acetate (0.025%) enhanced growth of Δ*glcB* in the presence of glucose. The metabolomics analysis revealed that at 0.025% acetate and 0.2% glucose, many of the metabolic changes observed in Δ*glcB* in 0.2% acetate and 0.2% glucose were absent or less severe, raising the possibility that *Mtb* has optimized its capacity for cocatabolism and growth around specific metabolic objectives distinct from other microbes (43).

Because of its importance in *Mtb* virulence, ICL has been the focus of multiple drug discovery efforts. However, to date, reports of potent and selective ICL inhibitors remain lacking (44, 45). This deficiency likely reflects the challenges associated with ICL's small active site, which is composed primarily of polar and charged side chains. In contrast, the structurally different active site of MS contains a mix of apolar and polar amino acids making it more druggable than ICL (20). The MS active site is a long (25 Å) cavity, with a diameter of about 9 Å, connecting the outside solvent to the Mg^{2+} in the catalytic center. The main function of the long tunnel is to bind the tail of acetyl CoA and position the acetyl group in the bottom of the cavity next to glyoxylate, which is coordinated to Mg^{2+} (46). Thus, the active site is considerably larger than the one of ICL and chemically more diverse, and it offers many opportunities for inhibitor binding.

The severe attenuation of MS-deficient *Mtb* in the mouse model is consistent with previous evidence that *Mtb* is exposed to fatty acids during acute and chronic mouse infections. This work further validates MS as a drug target in *Mtb* and encourages continued efforts to develop therapeutic MS inhibitors.

In summary, this study defines a previously unappreciated but essential physiologic role of MS as a metabolite detoxification enzyme in a human pathogen and highlights a generally underappreciated but potentially important dissociation between the conservation of a gene's biochemical and physiologic function.

Materials and Methods

Bacteria Culture Conditions. *Mtb* strains were cultured in Middlebrook 7H9 containing 0.5% fatty-acid–free BSA (Roche BSA fraction V, heat shock, fatty-acid–free with total FA ≤1.2 mg/g), 0.2% glucose, 0.085% NaCl, 0.2% glycerol, and 0.05% tyloxapol. For agar plates, Middlebrook 7H10 agar with 0.5% glycerol, 0.5% BSA fraction V (fatty-acid–free), 0.2% glucose, and 0.085% NaCl was used. For media containing oleic acid, 10% (vol/vol) commercial OADC (oleic acid, albumin, dextrose, catalase) supplement (final concentration 0.5% BSA, 0.2% glucose, 0.085% NaCl, 0.006% oleic acid, and 0.0003% catalase) and 0.5% glycerol was added to 7H9 or 7H10 media, prepared according to manufacturer's instructions. Carbon-defined minimal media consisted of 0.05% potassium phosphate monobasic, 0.05% magnesium sulfate heptahydrate, 0.2% citric acid, 0.005% ferric ammonium sulfate, 0.05% ammonium sulfate, 0.0001% zinc sulfate, and 0.05% tyloxapol. Carbon sources propionic acid, butyric acid, sodium acetate, valeric acid, glucose, and glycerol were added at the indicated concentration (%wt/vol or %vol/vol, depending on stock), and pH adjusted to 7.4. Growth curves with cholesterol were performed in "cholesterol base media" as previously described (26). Briefly, a 500× stock of cholesterol was made by addition of 100 mg cholesterol to 1 mL of tyloxapol and 1 mL of ethanol. This was heated to 95 °C–100 °C before addition to warm minimal media containing 0.5 g/L asparagine, 1 g/L KH_2PO_4, 2.5 g/L Na_2HPO_4, 0.05 g/L ferric ammonium citrate, 0.5 g/L $MgSO_4 \bullet 7H_2O$, 0.5 mg/L $CaCl_2$, and 0.1 mg/L $ZnSO_4$. Media was sterilized by filtration. When required, hygromycin B (50 μg/mL), streptomycin (10 μg/mL), kanamycin (25 μg/mL), and/or zeocin (25 μg/mL) were added. Where indicated, atc was added at 500 ng/mL and replenished at 250 ng/mL every 4–5 d. For metabolomics profiling, *Mtb* culture at OD_{580} ∼1 was seeded onto 0.22-μM nitrocellulose filters atop 7H10 agar plates containing 0.5% fatty-acid–free BSA, 0.085% NaCl, 0.2% glucose, and 0.5% glycerol for 4 d, then 0.2% glucose for 2 d, before transfer to the indicated carbon source for 1 d. Bacteria were subsequently quenched in cold LC-MS–grade acetonitrile:methanol:water (40:40:20) buffer, scraped off of filters, and mechanically lysed using a bead beater before metabolite analysis.

Generation of Mutant Strains. All mutant strains were generated in the *M. tuberculosis* Erdman background. *Mtb* was first transformed with an attL5-integrating plasmid expressing *glcB* under the control of its native promoter. In this merodiploid strain, the native copy of *glcB* was replaced with a hygromycin resistance by homologous recombination. This att-site mutant was then used to generate both the *glcB*-DUC and *glcB* knockout strains. To generate *glcB*-DUC, the att-site mutant was transformed with an att-site–integrating plasmid expressing *glcB* C-terminally tagged with DAS+4 under the control of a Tet-OFF promoter (P750) controlled by the tetracycline repressor T38S38, and also a tweety-site integrating plasmid expressing *sspB* under the control of a Tet-ON promoter (P1) controlled by TSC10M repressor as described (21). The *glcB* knockout strain (Δ*glcB*) was generated from the att-site mutant by replacement transformation of the *glcB*-expressing plasmid in the attL5 site with a plasmid lacking *glcB*. The complemented strain was generated by transforming Δ*glcB* with an attL5-site–integrating plasmid expressing *glcB* under the control of the native *glcB* promoter. All vectors used for mutant generation and complementation were constructed using Gateway Cloning Technology (Invitrogen).

Survival Assays. *Mtb* cultures were grown to OD 0.2–1 in supplemented 7H9 medium with 0.5% fatty-acid–free BSA, 0.2% glucose, 0.085% NaCl, 0.2% glycerol, and 0.05% tyloxapol and spun down to remove the media. Pellets were resuspended in carbon-defined minimal media and used to inoculate 10 mL of the media of interest at an OD of 0.01. Cultures were incubated nonshaking at 37 °C at 5% CO_2 in T25 vented flasks. Flasks were shaken to fully resuspend bacteria before aliquots were taken for serial dilutions and culture on 7H10 agar containing 0.5% fatty-acid–free BSA, 0.2% glucose, 0.085% NaCl, and 0.5% glycerol.

Metabolomics. LC-MS differentiation and detection of *Mtb* metabolites was performed with an Agilent Accurate Mass 6220 TOF coupled with an Agilent 1200 Liquid Chromatography system using a Cogent Diamond Hydride Type C column (Microsolve Technologies) as described (12). Standards of authentic chemicals of known amounts were mixed with bacterial lysates and analyzed to generate the standard curves used to quantify metabolite levels. Metabolite concentrations were normalized to biomass based on measurement of residual peptide content in individual samples using the Pierce BCA Protein Assay kit. Data were analyzed using Profinder B.06.00 software.

Mouse and Macrophage Infections. We isolated and infected bone-marrow–derived mouse macrophages as previously described (47). Aerosol infections of 7-wk-old female C57BL/6 mice (The Jackson Laboratory) were performed using a Glas-Col inhalation exposure system with early log phase *Mtb* cultures prepared as single-cell suspensions in PBS to deliver 100–200 bacilli per mouse. At the indicated time points, doxycycline food (2000 ppm; Research Diets) was administered in lieu of regular mouse chow for the rest of the

experiment. To quantify bacteria, serial dilutions of lung and spleen homogenates were cultured on 7H10 plates containing 10% fatty-acid–free BSA, 0.2% glucose, 0.085% NaCl, and 0.5% glycerol. The left lobe of the mouse lungs was fixed in 10% formalin in PBS and used for staining with hematoxylin and eosin. Procedures involving mice were performed as according to National Institutes of Health guidelines for housing and care of laboratory animals and were reviewed and approved by the Institutional Animal Care and Use Committee of Weill Cornell Medical College.

Immunoblot Analysis. Rabbit polyclonal antiserum against recombinant malate synthase protein (18) was generated by GenScript. Immunoblot analysis was done as described (24) using malate synthase antiserum (1:3,500) or antiserum against the proteasome subunit B (PrcB) (1:20,000) in Odyssey blocking buffer and PBS (1:1) in 0.1% Tween-20. The membranes were washed and then incubated with secondary IRDye 680 donkey anti-rabbit IgG (H+L) (LI-COR Biosciences). After washing, proteins were visualized using the Odyssey Infrared Imaging System (LI-COR Biosciences).

ACKNOWLEDGMENTS. We thank Natalia Betancourt, Alexandre Gouzy, Pradeepa Jayachandran, and Naomi Song for assistance with experiments; John D. McKinney for providing the Δ*icl1*Δ*icl2* mutant *Mtb* strain; Christopher Sassetti for the cholesterol medium protocol; and Gang Lin and Carl Nathan for PrcB-specific antiserum. This work was supported by NIH Grants R01 AI092573, T32 AI007621, and U19 AI111143 (Tri-Institutional TB Research Unit).

1. Ehrt S, Rhee K (2013) *Mycobacterium tuberculosis* metabolism and host interaction: Mysteries and paradoxes. *Curr Top Microbiol Immunol* 374:163–188.
2. Peyron P, et al. (2008) Foamy macrophages from tuberculous patients' granulomas constitute a nutrient-rich reservoir for M. tuberculosis persistence. *PLoS Pathog* 4(11):e1000204.
3. Kim M-J, et al. (2010) Caseation of human tuberculosis granulomas correlates with elevated host lipid metabolism. *EMBO Mol Med* 2(7):258–274.
4. Muñoz-Elías EJ, McKinney JD (2005) *Mycobacterium tuberculosis* isocitrate lyases 1 and 2 are jointly required for in vivo growth and virulence. *Nat Med* 11(6):638–644.
5. Pandey AK, Sassetti CM (2008) Mycobacterial persistence requires the utilization of host cholesterol. *Proc Natl Acad Sci USA* 105(11):4376–4380.
6. Marrero J, Rhee KY, Schnappinger D, Pethe K, Ehrt S (2010) Gluconeogenic carbon flow of tricarboxylic acid cycle intermediates is critical for *Mycobacterium tuberculosis* to establish and maintain infection. *Proc Natl Acad Sci USA* 107(21):9819–9824.
7. Blumenthal A, Trujillo C, Ehrt S, Schnappinger D (2010) Simultaneous analysis of multiple *Mycobacterium tuberculosis* knockdown mutants in vitro and in vivo. *PLoS One* 5(12):e15667.
8. Ganapathy U, et al. (2015) Two enzymes with redundant fructose bisphosphatase activity sustain gluconeogenesis and virulence in *Mycobacterium tuberculosis*. *Nat Commun* 6:7912.
9. Murima P, McKinney JD, Pethe K (2014) Targeting bacterial central metabolism for drug development. *Chem Biol* 21(11):1423–1432.
10. Griffin JE, et al. (2011) High-resolution phenotypic profiling defines genes essential for mycobacterial growth and cholesterol catabolism. *PLoS Pathog* 7(9):e1002251.
11. Munoz-Elias EJ (2005) The role of the glyoxylate cycle in the pathogenesis of *Mycobacterium tuberculosis*. PhD thesis (The Rockefeller University, New York, NY). Available at digitalcommons.rockefeller.edu/student_theses_and_dissertations/55/. Accessed February 18, 2017.
12. Eoh H, Rhee KY (2013) Multifunctional essentiality of succinate metabolism in adaptation to hypoxia in *Mycobacterium tuberculosis*. *Proc Natl Acad Sci USA* 110(16):6554–6559.
13. Eoh H, Rhee KY (2014) Methylcitrate cycle defines the bactericidal essentiality of isocitrate lyase for survival of *Mycobacterium tuberculosis* on fatty acids. *Proc Natl Acad Sci USA* 111(13):4976–4981.
14. Gengenbacher M, Rao SPS, Pethe K, Dick T (2010) Nutrient-starved, non-replicating *Mycobacterium tuberculosis* requires respiration, ATP synthase and isocitrate lyase for maintenance of ATP homeostasis and viability. *Microbiology* 156(Pt 1):81–87.
15. Nandakumar M, Nathan C, Rhee KY (2014) Isocitrate lyase mediates broad antibiotic tolerance in *Mycobacterium tuberculosis*. *Nat Commun* 5:4306.
16. Muñoz-Elías EJ, Upton AM, Cherian J, McKinney JD (2006) Role of the methylcitrate cycle in *Mycobacterium tuberculosis* metabolism, intracellular growth, and virulence. *Mol Microbiol* 60(5):1109–1122.
17. Gould TA, van de Langemheen H, Muñoz-Elías EJ, McKinney JD, Sacchettini JC (2006) Dual role of isocitrate lyase 1 in the glyoxylate and methylcitrate cycles in *Mycobacterium tuberculosis*. *Mol Microbiol* 61(4):940–947.
18. Smith CV, et al. (2003) Biochemical and structural studies of malate synthase from *Mycobacterium tuberculosis*. *J Biol Chem* 278(3):1735–1743.
19. Quartararo CE, Blanchard JS (2011) Kinetic and chemical mechanism of malate synthase from *Mycobacterium tuberculosis*. *Biochemistry* 50(32):6879–6887.
20. Krieger IV, et al. (2012) Structure-guided discovery of phenyl-diketo acids as potent inhibitors of *M. tuberculosis* malate synthase. *Chem Biol* 19(12):1556–1567.
21. Kim J-H, et al. (2013) A genetic strategy to identify targets for the development of drugs that prevent bacterial persistence. *Proc Natl Acad Sci USA* 110(47):19095–19100.
22. Pashley CA, Parish T (2003) Efficient switching of mycobacteriophage L5-based integrating plasmids in *Mycobacterium tuberculosis*. *FEMS Microbiol Lett* 229(2):211–215.
23. Trujillo C, et al. (2014) Triosephosphate isomerase is dispensable in vitro yet essential for *Mycobacterium tuberculosis* to establish infection. *mBio* 5(2):e00085–14.
24. Puckett S, et al. (2014) Inactivation of fructose-1,6-bisphosphate aldolase prevents optimal co-catabolism of glycolytic and gluconeogenic carbon substrates in *Mycobacterium tuberculosis*. *PLoS Pathog* 10(5):e1004144.
25. Zhang YJ, et al. (2012) Global assessment of genomic regions required for growth in *Mycobacterium tuberculosis*. *PLoS Pathog* 8(9):e1002946.
26. Griffin JE, et al. (2012) Cholesterol catabolism by *Mycobacterium tuberculosis* requires transcriptional and metabolic adaptations. *Chem Biol* 19(2):218–227.
27. Savvi S, et al. (2008) Functional characterization of a vitamin B12-dependent methylmalonyl pathway in *Mycobacterium tuberculosis*: Implications for propionate metabolism during growth on fatty acids. *J Bacteriol* 190(11):3886–3895.
28. Meany JE, Pocker Y (1991) The dehydration of glyoxalate hydrate: General-acid, general-base, metal ion and enzymic catalysis. *J Am Chem Soc* 113(16):6155–6161.
29. Salido E, Pey AL, Rodriguez R, Lorenzo V (2012) Primary hyperoxalurias: Disorders of glyoxylate detoxification. *Biochim Biophys Acta* 1822(9):1453–1464.
30. Ruffo A, Testa E, Adinolfi A, Pelizza G, Moratti R (1967) Control of the citric acid cycle by glyoxylate. Mechanism of the inhibition by oxalomalate and gamma-hydroxy-alpha-oxoglutarate. *Biochem J* 103(1):19–23.
31. Dangelmaier CA, Holmsen H (2014) Glyoxylate lowers metabolic ATP in human platelets without altering adenylate energy charge or aggregation. *Platelets* 25(1):36–44.
32. Beatty SM, Hamilton GA (1985) Inhibition of pyruvate dehydrogenase and pyruvate dehydrogenase phosphate phosphatase by glyoxylate. *Bioorg Chem* 13(1):14–23.
33. Payes B, Laties GG (1963) The inhibition of several tricarboxylic acid cycle enzymes by γ-hydroxy- α-ketoglutarate. *Biochem Biophys Res Commun* 10(6):460–466.
34. Johanson RA, Reeves HC (1977) Concerted inhibition of NADP+-specific isocitrate dehydrogenase by oxalacetate and glyoxylate. I. Oxalomalate formation and stability, and nature of the enzyme inhibition. *Biochim Biophys Acta* 483(1):24–34.
35. Höner Zu Bentrup K, Miczak A, Swenson DL, Russell DG (1999) Characterization of activity and expression of isocitrate lyase in Mycobacterium avium and *Mycobacterium tuberculosis*. *J Bacteriol* 181(23):7161–7167.
36. Berg JM, Tymoczko JL, Stryer L (2006) Biochemistry (W. H. Freeman, New York).
37. Evans JC, et al. (2016) Validation of CoaBC as a bactericidal target in the coenzyme A pathway of *Mycobacterium tuberculosis*. *ACS Infect Dis* 2(12):958–968.
38. Vereecke D, et al. (2002) Chromosomal locus that affects pathogenicity of *Rhodococcus fascians*. *J Bacteriol* 184(4):1112–1120.
39. Zahoor A, Otten A, Wendisch VF (2014) Metabolic engineering of *Corynebacterium glutamicum* for glycolate production. *J Biotechnol* 192(Pt B):366–375.
40. Cusa E, Obradors N, Baldomà L, Badía J, Aguilar J (1999) Genetic analysis of a chromosomal region containing genes required for assimilation of allantoin nitrogen and linked glyoxylate metabolism in *Escherichia coli*. *J Bacteriol* 181(24):7479–7484.
41. Giffin MM, Modesti L, Raab RW, Wayne LG, Sohaskey CD (2012) ald of *Mycobacterium tuberculosis* encodes both the alanine dehydrogenase and the putative glycine dehydrogenase. *J Bacteriol* 194(5):1045–1054.
42. Murima P, et al. (2016) A rheostat mechanism governs the bifurcation of carbon flux in mycobacteria. *Nat Commun* 7:12527.
43. de Carvalho LPS, et al. (2010) Metabolomics of *Mycobacterium tuberculosis* reveals compartmentalized co-catabolism of carbon substrates. *Chem Biol* 17(10):1122–1131.
44. Sacchettini JC, Rubin EJ, Freundlich JS (2008) Drugs versus bugs: In pursuit of the persistent predator *Mycobacterium tuberculosis*. *Nat Rev Microbiol* 6(1):41–52.
45. Lee Y-V, Wahab HA, Choong YS (2015) Potential inhibitors for isocitrate lyase of *Mycobacterium tuberculosis* and non-M. tuberculosis: A summary. *BioMed Res Int* 2015:895453.
46. Huang H-L, Krieger IV, Parai MK, Gawandi VB, Sacchettini JC (2016) *Mycobacterium tuberculosis* malate synthase structures with fragments reveal a portal for substrate/product exchange. *J Biol Chem* 291(53):27421–27432.
47. Vandal OH, Pierini LM, Schnappinger D, Nathan CF, Ehrt S (2008) A membrane protein preserves intrabacterial pH in intraphagosomal *Mycobacterium tuberculosis*. *Nat Med* 14(8):849–854.